

Apparent Non-Double-Couple Components as Artifacts of Moment Tensor Inversion

Boris Rösler *, Seth Stein , Adam T. Ringler , Jiří Vackář 

¹Department of Earth and Planetary Sciences, Northwestern University, Evanston, Illinois, U.S.A., ²now at Center for Scientific Research and Higher Education at Ensenada (CICESE), Ensenada, Mexico, ³Institute for Policy Research, Northwestern University, Evanston, Illinois, U.S.A., ⁴Albuquerque Seismological Laboratory, United States Geological Survey, Albuquerque, New Mexico, U.S.A., ⁵Institute of Rock Structure and Mechanics, Czech Academy of Sciences, Prague, Czech Republic

Author contributions: *Conceptualization:* Boris Rösler. *Methodology:* Boris Rösler, Seth Stein. *Software:* Boris Rösler, Adam T. Ringler, Jiří Vackář. *Validation:* Seth Stein. *Formal Analysis:* Boris Rösler, Seth Stein. *Writing - Original draft:* Boris Rösler. *Writing - Review & Editing:* Seth Stein, Adam T. Ringler, Jiří Vackář.

Abstract Compilations of earthquake moment tensors from global and regional catalogs find pervasive non-double-couple (NDC) components with a mean deviation from a double-couple (DC) source of around 20%. Their distributions vary only slightly with magnitude, faulting mechanism, or geologic environments. This consistency suggests that for most earthquakes, especially smaller ones whose rupture processes are expected to be simpler, the NDC components are largely artifacts of the moment tensor inversion procedure. This possibility is also supported by the fact that NDC components for individual earthquakes with $M_w < 6.5$ are only weakly correlated between catalogs. We explore this possibility by generating synthetic seismograms for the double-couple components of earthquakes around the world using one Earth model and inverting them with a different Earth model. To match the waveforms with a different Earth model, the inversion changes the mechanisms to include a substantial NDC component while largely preserving the fault geometry (DC component). The resulting NDC components have a size and distribution similar to those reported for the earthquakes in the Global Centroid Moment Tensor (GCMT) catalog. The fact that numerical experiments replicate general features of the pervasive NDC components reported in moment tensor catalogs implies that these components are largely artifacts of the inversions not adequately accounting for the effects of laterally varying Earth structure.

Production Editor:
Gareth Funning
Handling Editor:
Stephen Hicks
Copy & Layout Editor:
Ethan Williams

Received:
23 November 2023
Accepted:
5 March 2024
Published:
4 April 2024

1 Introduction

Moment tensors (MTs) are a general description of earthquake sources, providing information beyond a double-couple (DC) force system representing slip on a fault plane (Gilbert, 1971). The deployment of global digital seismic networks allowed development of large catalogs of moment tensors (e.g., Ekström et al. 2012). These catalogs have become an important tool in studies worldwide, including analyzing global plate motions and deformation in plate boundary zones and within plates.

As MT catalogs were developed (Dziewonski et al., 1981), it became clear that many earthquakes showed non-double-couple (NDC) components whose origin became a topic of investigation (Sipkin, 1986; Frohlich, 1994). This effect is evident along many plate boundaries (Fig. 1). For example, along the Mid-Atlantic ridge, many earthquake mechanisms deviate from the DC mechanisms for pure strike-slip on transforms and normal faulting on ridge segments (Tréhu et al., 1981).

A NDC component is identified by decomposing a moment tensor. Diagonalization of the MT yields a tensor with eigenvalues λ_1 , λ_2 and λ_3 on its diagonal, where $\lambda_1 > \lambda_3 > \lambda_2$. Subtracting a diagonal matrix with components equal to the isotropic moment $M_0^{iso} =$

$(\lambda_1 + \lambda_2 + \lambda_3)/3$, representing the source's volumetric change, yields the deviatoric moment tensor typically reported in catalogs. The deviatoric MT has no net volume change because its trace, the sum of its eigenvalues, $\lambda'_1 + \lambda'_2 + \lambda'_3 = 0$.

The decomposition of this deviatoric MT into a DC and a NDC component (Knopoff and Randall, 1970) describes the NDC component as a compensated linear vector dipole (CLVD), three force dipoles with one twice the magnitude of the others, yielding no volume change,

$$\begin{pmatrix} \lambda'_1 & 0 & 0 \\ 0 & \lambda'_2 & 0 \\ 0 & 0 & \lambda'_3 \end{pmatrix} = (\lambda'_1 + 2\lambda'_3) \begin{pmatrix} 1 & 0 & 0 \\ 0 & -1 & 0 \\ 0 & 0 & 0 \end{pmatrix} + \lambda'_3 \begin{pmatrix} -2 & 0 & 0 \\ 0 & 1 & 0 \\ 0 & 0 & 1 \end{pmatrix}. \quad (1)$$

For a pure double couple, $\lambda'_3 = 0$ and $\lambda'_1 = -\lambda'_2$. The ratio of the smallest and absolutely largest eigenvalues

$$|\epsilon| = \frac{|\lambda'_3|}{\max(|\lambda'_1|, |\lambda'_2|)} \quad (2)$$

quantifies the size of the NDC component, the deviation from a DC source (Dziewonski et al., 1981).

NDC components can arise in several ways. Some appear to reflect intrinsically complex source processes

*Corresponding author: boris@earth.northwestern.edu

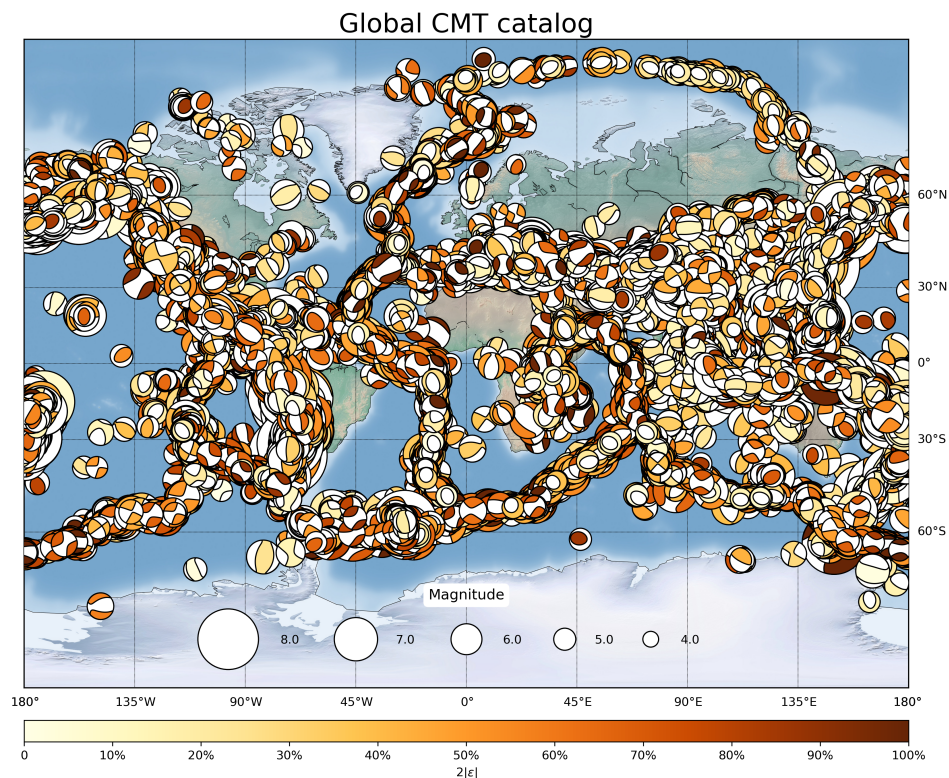


Figure 1 The source mechanisms of the 62337 earthquakes in the Global Centroid Moment Tensor (GCMT) catalog between 1976 and 2022. Many mechanisms show a substantial non-double couple (NDC) component.

that differ from slip on a planar fault for earthquakes in specific geologic environments, notably volcanic areas (e.g., Kanamori and Given, 1982; Ross et al., 1996; Nettles and Ekström, 1998; Shuler et al., 2013a,b; Gudmundsson et al., 2016; Sandanbata et al., 2021; Rodríguez-Cardozo et al., 2021). Others are additive, reflecting the combined effect of near-simultaneous rupture on multiple faults with different geometries (e.g., Kawakatsu, 1991; Hayes et al., 2010; Hamling et al., 2017; Scognamiglio et al., 2018; Yang et al., 2021; Ruhl et al., 2021), or a rupture with changes in geometry (Wald and Heaton, 1994; Cohee and Beroza, 1994; Pang et al., 2020). Alternatively, they may be artifactual (McNamara et al., 2013; Ammon et al., 1994), results of the inversion without geologic meaning, generated by noise in the waveforms (Šílený et al., 1996; Jechumtálová and Šílený, 2001), inappropriate seismic station coverage (Cesca et al., 2006; Ford et al., 2010; Vera Rodriguez et al., 2011; Domingues et al., 2013), or not accounting for laterally varying Earth structure during the inversion (Šílený, 2004; Cesca et al., 2006; Rössler et al., 2007).

By comparing MTs in the Global CMT Project (GCMT) and U.S. Geological Survey (USGS) catalogs, Rössler et al. (2021) found that the distribution (e.g., mean and standard deviation) of NDC components in different catalogs are quite similar. However, the actual values are only weakly correlated for events with $M_w < 6.5$. Because the catalogs use different inversion procedures, the poor correlation between the NDC components suggests that they are artifacts. Moreover, using a large dataset compiled from multiple global and regional MT catalogs, Rössler and Stein (2022) found that for earthquakes with magnitudes $2.9 < M_w < 8.2$, NDC compo-

nents are common, with an average value of $2|\epsilon| = 23.2\%$ that varies only slightly with magnitude. They argued that this consistency indicates that NDC components are unlikely to reflect rupture on multiple faults, which is more likely to occur for large earthquakes (Quigley et al., 2017). They also found only small differences in NDC components between earthquakes with different faulting mechanisms, or in different geologic environments. These results are interesting in that NDC components are often assumed to be most likely in volcanic and thus extensional environments (Ross et al., 1996; Julian and Sipkin, 1985; Miller et al., 1998; Nettles and Ekström, 1998). Hence the consistency suggests that for most earthquakes, especially smaller ones, the NDC components do not reflect complex rupture processes and are therefore artifacts of the moment tensor inversion.

Studies have identified the influence of Earth structure on moment tensor inversions (Henry et al., 2002; Hjörleifsdóttir and Ekström, 2010), and attempts have been made to reduce the uncertainties introduced by lateral heterogeneity in the Earth in inversions based on one-dimensional (1D) Earth models (Vasyura-Bathke et al., 2021; Phạm and Tkalčić, 2021). Apart, moment tensor solutions based on Green's functions generated for three-dimensional (3D) Earth models for regional earthquakes have been calculated (Hingee et al., 2011; Hejrani et al., 2017; Zhu and Zhou, 2016; Wang and Zhan, 2020; Liu et al., 2004; Jechumtálová and Bulant, 2014; Covellone and Savage, 2012), which, in some cases, were improved using rotational motions (Donner et al., 2020). Sawade et al. (2022) compiled the CMT3D moment tensor catalog for global earthquakes with M_w

≥ 5.5 using a 3D Earth model for the inversion. Its NDC components are smaller on average than the ones in the GCMT catalog, showing how spurious NDC components can be reduced in inversions accounting for lateral variations in the structure of the Earth.

The availability of multiple moment tensor catalogs with different inversion procedures allows us to quantify this phenomenon on a global scale, and we explore whether the distribution of NDC components can be generated by the MT inversion process by generating synthetic seismograms for pure DC source processes and invert them using an approach that simulates the effect of uncertainties in the Earth structure assumed for the inversion.

2 Methodology

For our study, we model earthquakes selected from the Global Centroid Moment Tensor (GCMT) catalog, which contains about 60,000 earthquakes since 1976 (Ekström et al., 2012). We classify earthquakes by their faulting type, following Frohlich (1992). We calculate the plunge of the P- (most compressive), N- (null), and T-axes (least compressive) from the eigenvectors of the moment tensors. An earthquake is considered a normal faulting earthquake if its P-axis plunge satisfies $\sin^2 \delta_P \geq 2/3$ ($\delta_P \geq 54.75^\circ$), strike-slip if its N-axis plunge exceeds 54.75° , and a thrust fault if its T-axis plunge exceeds 54.75° (Saloor and Okal, 2018). If the plunge of none of the axes exceeds the threshold, an earthquake is considered oblique faulting. Of the earthquakes in the catalog up to the year 2022, 34.9% have thrust mechanisms, 24.5% are strike-slip, 22.2% have normal faulting mechanisms, and 18.4% have oblique-faulting mechanisms. We therefore model nine earthquakes with thrust mechanisms, six with strike-slip mechanisms, five with normal faulting mechanisms, and five with oblique faulting mechanism, consistent with the fractions in the GCMT catalog. We choose these 25 earthquakes as representative of the geologic environment they occurred in, with a geographical distribution over all continents to avoid bias due to Earth's elliptical shape and its rotation (Fig. 2). 22 of them have depths of less than 30km, similar to the vast majority of earthquakes in the GCMT catalog. To avoid magnitude bias, we model the earthquakes with a moment magnitude of $M_w 7.0$, which ensures that they are detected at stations around the world, but can be modeled as a point source.

The one-dimensional Preliminary Reference Earth model (PREM, Dziewonski and Anderson, 1981) is used by the three global MT catalogs of the Global CMT Project (Dziewonski et al., 1981; Ekström et al., 2012), the USGS (Hayes et al., 2009) and the Deutsches GeoForschungsZentrum (GFZ, Joachim Saul, personal communication, 2022) in their inversion procedure. To simulate the deviation of the Earth model used in the inversion from the actual Earth structure, we perturb the one-dimensional model for the generation of synthetic seismograms. We calculate synthetic seismograms by way of normal mode summation for a spherically symmetric non-rotating Earth and include the effects of attenuation and self-gravitation for both the spheroidal

and toroidal components from angular order 0 to 8000 with a period range of 0 to 20 mHz and a sampling rate of 1/s. The first 200 dispersion branches are also included in the synthetic seismogram calculation, and the moment tensor is incorporated by convolving the eigenfunctions with the moment tensor components obtained for the DC component from the MTs as reported in the GCMT catalog. We then invert them using Green's functions generated for the unperturbed PREM model. Any NDC component in the resulting moment tensors is thus an artifact of the inversion resulting from the difference in Earth structure. This process simulates current methodology for global catalogs in which MTs are found using one-dimensional (laterally homogeneous) Earth models. Although ideally the analysis would involve generating and inverting seismograms for three-dimensional (laterally varying) Earth models, our approach using a range of perturbations allows quantifying the effect of laterally varying Earth structure in the inversion.

We perturb the elastic and anelastic structures of the Earth model independently while retaining the elastic moduli K , the bulk modulus, and μ , the shear modulus (Dahlen and Tromp, 1998, Section 3.6.2) in each layer from the PREM model. We determine μ and K from the PREM P- and S-wave velocities v_{pv} and v_{sv} , and density ρ using

$$\begin{aligned} v_{sv} &= \sqrt{\frac{K}{\mu}} \Rightarrow \mu = v_{sv}^2 \rho \\ v_{pv} &= \sqrt{\frac{K + \frac{4}{3}\mu}{\rho}} \Rightarrow K = \rho (v_{pv}^2 - \frac{4}{3}v_{sv}^2). \end{aligned} \quad (3)$$

Next, we perturb the P-wave velocity v_{pv} by randomly choosing its value from a Gaussian distribution with mean v_{pv} and standard deviation 1, 3, 5, and 10%, which reflect the uncertainties in the velocities (Dalton and Ekström, 2006). Keeping K and μ constant, we then determine the new density in each layer as

$$\rho_{new} = \frac{K + \frac{4}{3}\mu}{v_{pv, new}^2} \quad (4)$$

from which we determine the new S-wave velocity as

$$v_{sv} = \sqrt{\frac{\mu}{\rho_{new}}}. \quad (5)$$

Of the 185 layers in the model PREM, nine in the upper mantle are anisotropic. For those, η (Dahlen and Tromp, 1998, Section 8.9) which relates the horizontal P-wave velocity to the vertical S-wave velocity is given,

$$\eta = \frac{F}{\rho_{old} (v_{ph, old}^2 - 2v_{sv, old}^2)}, \quad (6)$$

from which we obtain $F = \eta \rho_{old} (v_{ph, old}^2 - 2v_{sv, old}^2)$. The new horizontal P-wave velocity is then

$$v_{ph, new} = \sqrt{\frac{F}{\eta \rho_{new}} + 2v_{sv, new}^2}. \quad (7)$$

Earthquakes and seismic stations

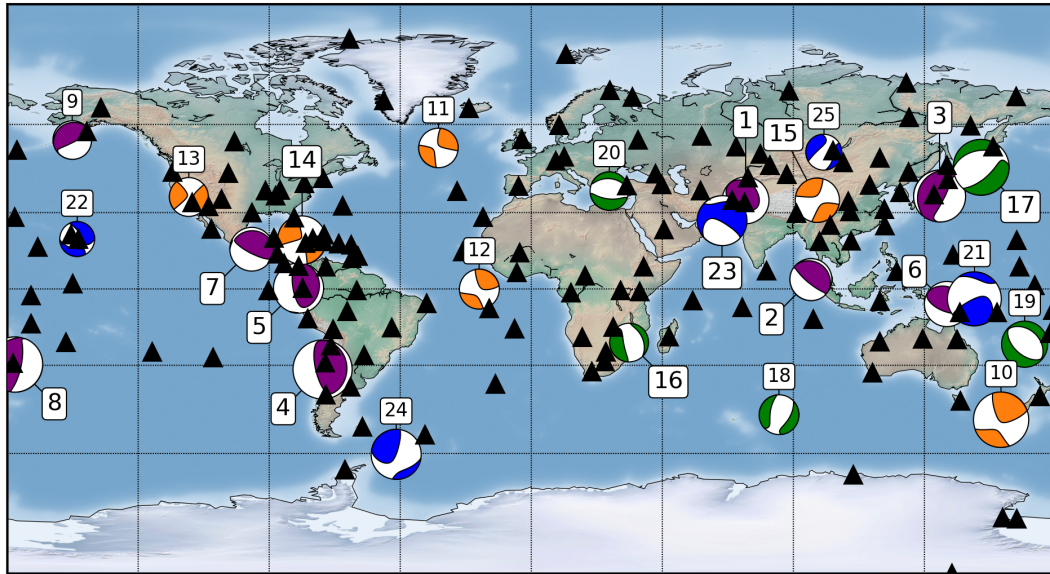


Figure 2 Earthquakes and seismic stations used in this study. The location and origin time of the earthquakes are listed in Table 1. Consistent with the fractions in the Global Centroid Moment Tensor (GCMT) catalog, nine of the 25 earthquakes have a thrust faulting mechanism, six have a strike-slip faulting mechanism, five have a normal faulting mechanism, and 5 have an oblique faulting mechanism. The 150 seismic stations in the Global Seismographic Network (GSN) network provide good worldwide station coverage.

Number	Date	Time	Latitude	Longitude	Depth	M_w	Faulting Type
1	2005-10-08	03:50:40.8	34.54	73.59	12.0	7.58	thrust
2	2010-05-09	05:59:41.6	3.75	96.02	37.2	7.25	thrust
3	2011-03-11	06:15:45.0	36.13	140.23	29.0	7.89	thrust
4	2015-09-16	22:54:32.9	-31.57	-71.67	17.4	8.27	thrust
5	2016-04-16	23:58:36.9	0.35	-79.93	22.3	7.78	thrust
6	2018-02-25	17:44:44.1	-6.07	142.75	12.0	7.47	thrust
7	2020-06-23	15:29:04.3	15.88	-96.01	21.5	7.38	thrust
8	2021-03-04	19:28:33.2	-29.72	-177.28	33.9	8.07	thrust
9	2021-08-14	11:57:43.5	55.18	-157.64	25.0	7.00	thrust
10	2004-12-23	14:59:04.4	-49.31	161.35	27.5	8.08	strike-slip
11	2015-02-13	18:59:12.2	52.65	-31.9	25.2	7.07	strike-slip
12	2016-08-29	04:29:57.9	-0.05	-17.83	26.8	7.10	strike-slip
13	2019-07-06	03:19:53.0	35.77	-117.6	12.0	7.03	strike-slip
14	2020-01-28	19:10:24.9	19.42	-78.76	23.9	7.69	strike-slip
15	2021-05-21	18:04:13.6	34.59	98.24	12.0	7.42	strike-slip
16	2006-02-22	22:19:07.8	-21.32	33.58	12.0	7.01	normal
17	2007-01-13	04:23:21.2	46.24	154.52	12.0	8.10	normal
18	2015-12-04	22:25:00.1	-47.62	85.09	28.9	7.10	normal
19	2018-12-05	04:18:08.4	-21.95	169.43	17.8	7.53	normal
20	2020-10-30	11:51:27.4	37.91	26.78	12.0	6.99	normal
21	2000-11-16	04:54:56.7	-3.98	152.17	24.0	8.00	oblique
22	2006-10-15	17:07:49.2	19.88	-155.93	48.0	6.71	oblique
23	2013-09-24	11:29:48.0	26.97	65.52	12.0	7.70	oblique
24	2013-11-17	09:04:55.5	-60.27	-46.4	23.8	7.78	oblique
25	2021-01-11	21:32:59.0	51.28	100.44	13.9	6.79	oblique

Table 1 List of earthquakes used in this study as reported in the GCMT catalog, indicating their origin time, location, depths, magnitude, and faulting type.

The new horizontal S-wave velocity v_{sh} is not restricted by the elastic constants and can thus be perturbed independently, similarly to the vertical P-wave velocity v_{pv} . Because the values related to anelastic structure are much less understood than the elastic structure (Karaoğlu and Romanowicz, 2018), the anelas-

tic structure is perturbed by randomly choosing a value from Gaussian distributions whose means, $1/Q_\kappa$ and $1/Q_\mu$, are the inverse of the original P- and S- wave quality factors, and whose standard deviations of 25, 50, and 75% thereof are typical for the variations found in attenuation tomography studies (e.g., Dalton and Ekström,

Comparison of perturbed Earth models to PREM

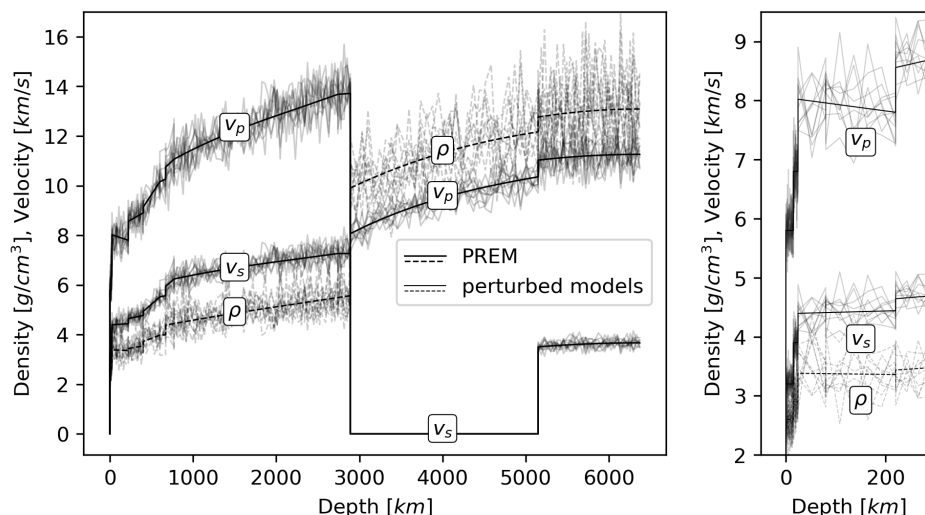


Figure 3 Comparison of the elastic structure of the Earth models used in this study, based on perturbation of model Preliminary Reference Earth Model (PREM)

2006).

Using these perturbed Earth models (Fig. 3), we generate three-component seismograms for the 150 stations of the Global Seismographic Network (GSN, Ringler et al., 2022) from one hour before the event time until 8000 s after it. This guarantees that the surface waves are included in the synthetic seismograms for all stations. For each earthquake we use the fifty closest stations which have an epicentral distance of at least 10° to avoid near-source effects (Aki and Richards, 2002).

To invert the seismograms, we use Green's functions generated for the unperturbed PREM model and perform a least-squares centroid MT inversion in a Bayesian framework using BayesISOLA (Vackář et al., 2017). BayesISOLA finds the moment tensor elements that give the best-fitting match to the synthetic seismograms in a full-waveform inversion from a linear combination of the Green's functions with the moment tensor elements as coefficients. We use frequencies from 0.002 to 0.01 Hz (i.e., periods between 100 and 500 s), as commonly used for global moment tensor inversions of large earthquakes (Ekström et al., 2012; Duputel et al., 2018; Kanamori and Rivera, 1993; Kanamori, 2008; Hayes et al., 2009), and the covariance matrix of Green's functions (Hallo and Gallovič, 2016) to estimate the effects of uncertainty in the Earth model. We fix the centroid location to the point for which the synthetic seismograms are generated but invert for centroid time in the range of ± 15 s about the centroid time of the synthetic event. We do not allow station-specific time delays as used in the inversion procedures of the GCMT catalog (Dziewonski et al., 1984). BayesISOLA calculates the best solution for the moment tensor as well as the posterior probability density function describing the uncertainty of the MT elements. Although the uncertainty might be useful to distinguish whether resulting NDC components are real or artifacts of the inversion, we only use the best solution in the comparison of the results with GCMT catalog, similar to the reported

MTs in this catalog.

Similar to the procedure of the GCMT catalog, we constrain the isotropic component of the MTs during the inversion so that the resulting MTs are purely deviatoric ($\lambda'_1 + \lambda'_2 + \lambda'_3 = 0$). However, in contrast to the GCMT procedure, we use longer period seismic waves. GCMT uses surface waves between 50 s and 150 s and mantle waves between 125 s and 350 s (Ekström et al., 2012). We do not use surface-waves delay dispersion maps, but the inversion procedures are comparable in most of parameters.

3 Results

Figure 4 shows an example of the seismic waveforms generated for the DC component of earthquake 12 in figure 2 at station II.SUR in Sutherland, South Africa, for a perturbed Earth model. Inversion of these seismograms using the unperturbed model PREM results in a moment tensor with an 8.7% artifactual NDC component, such that the waveforms generated for the resulting MT are nearly indistinguishable from those generated for the DC MT and the perturbed Earth model. Thus inversion with a different Earth model changes the mechanism to best match the waveforms at all stations by introducing a substantial NDC component. Repeating the process twelve times using different perturbed models to generate synthetic seismograms and inverting them with the unperturbed model yields a range of focal mechanisms (Fig. 5) with varying artifactual NDC components, averaging 4.4% for a perturbation of 5% in the elastic structure.

The DC component of the MT — the fault geometry — is generally retrieved well, as measured by the angle Φ in space required to rotate one set of a moment tensor's principal axes into the ones of another (Kagan, 1991). The angles are generally small, with an average value of 7.8° , less than the differences between moment tensors of the GCMT and the USGS for earthquakes of this mag-

Mid-Atlantic Ridge Earthquake

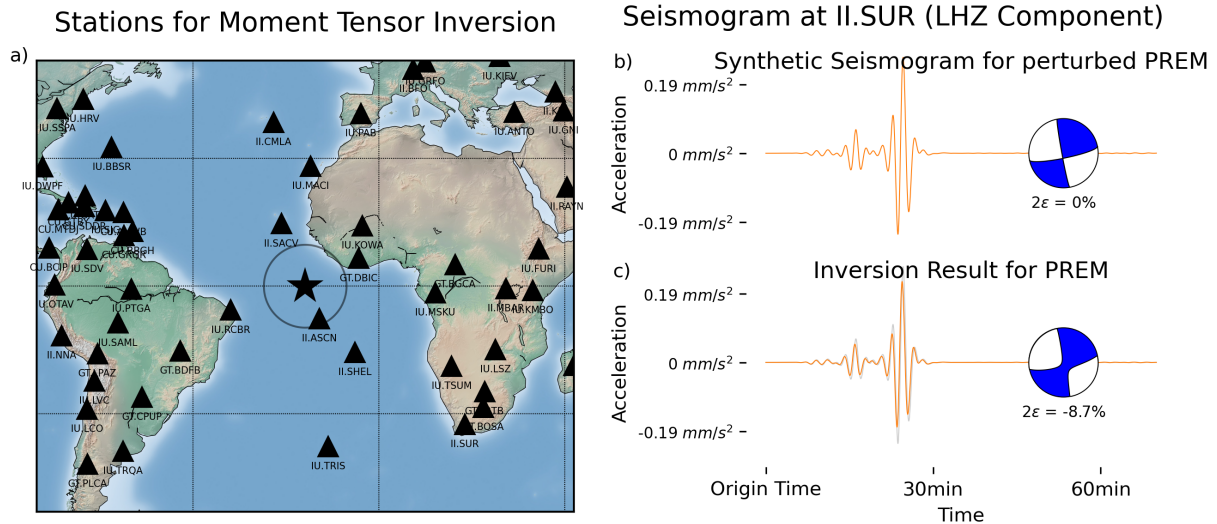


Figure 4 a) Stations for the moment tensor inversion of synthetic seismograms generated for the mid-Atlantic ridge earthquake of March 14, 1994. We used the fifty closest stations of the GSN network with an epicentral distance of at least 10° . b) Synthetic seismogram at station II.SUR (Sutherland, South Africa) generated for the DC component of the moment tensor for a perturbed model PREM with standard deviation of 5% in the seismic velocities with periods of 100 to 500 s. c) Synthetic seismogram generated for the moment tensor resulting from the inversion performed using Green’s functions generated for the unperturbed model PREM, compared to the input synthetic seismogram in b). Matching the waveform produces a spurious NDC component.

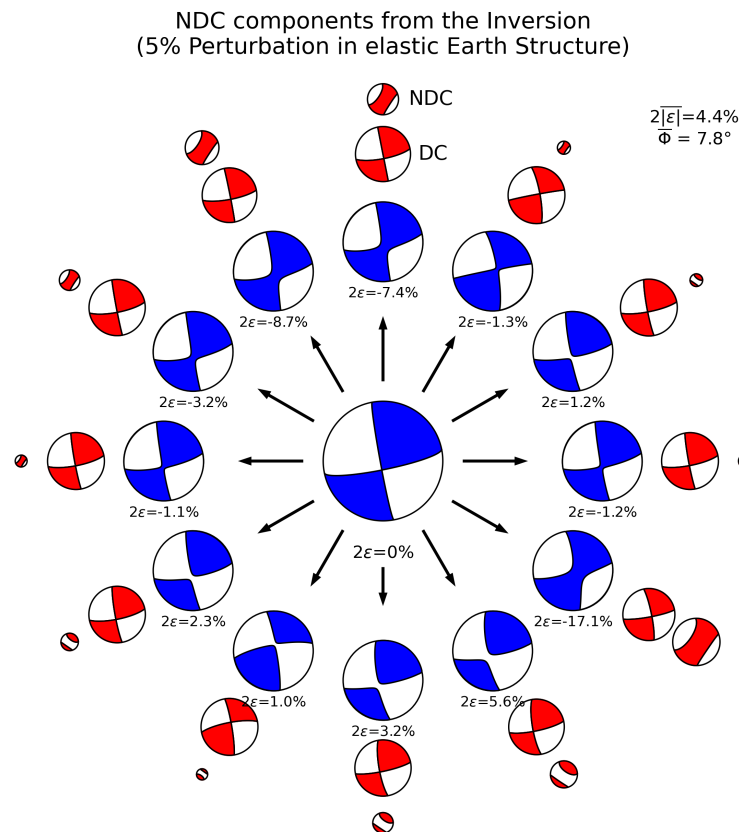


Figure 5 Inversion results for the mid-Atlantic ridge earthquake of March 14, 1994. Synthetic seismograms were generated for a pure double-couple (DC) mechanism and twelve different perturbed models based on Preliminary Reference Earth Model (PREM) and inverted using the unperturbed model. The resulting moment tensors (MTs) have very similar DC components, but substantial non-double couple (NDC) components (shown as twice as large) that differ in polarity and size.

Moment Tensor Inversion Results

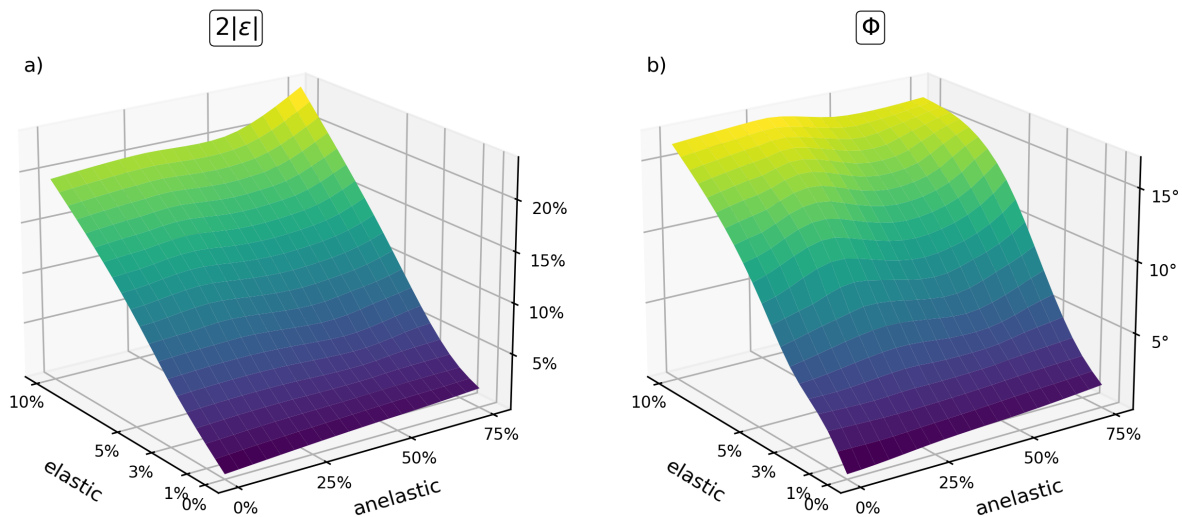


Figure 6 Inversion results for five inversions of each of the 25 earthquakes with five different perturbations of the elastic, and four different inversions of the anelastic structure. a) The resulting non-double-couple (NDC) components (2ϵ) depend primarily on the perturbation of the elastic Earth structure, with anelastic structure having little influence on the size of the NDC components. b) The angle required to rotate one moment tensor's set of principal axes into another (Φ) shows similar dependence on perturbations of the elastic and anelastic structure. The fault geometry is retrieved well, with rotation angles generally being smaller than 20° .

nitide (Rösler et al., 2021). However, the NDC components vary significantly in polarity and in size between -17.1 and 5.6%.

Carrying out five inversions for each of the 25 earthquakes with five different perturbations of the elastic and four perturbations of the anelastic structure each yields 2500 inversions. The resulting NDC components depend primarily on the perturbation of the elastic structure of the Earth model (Fig. 6a). Similarly, the deviation in fault geometry (Fig. 6b) depends little on the perturbation of the anelastic structure, further illustrating the relative importance of elastic and anelastic Earth structure on seismic waveforms (Dahlen, 1982). The values for the rotation angle are generally small, indicating that the DC component is recovered relatively accurately by inversions that poorly represent the actual Earth structure, whereas the NDC components have large uncertainties and are often artifacts of the inversion.

The NDC components reported in the GCMT catalog average 23.5% for all earthquakes. However, earthquakes with $M_w > 6.5$ have, on average, smaller NDC components (17.2%), which are determined with greater precision (Rösler et al., 2021, 2023). The NDC components in our experiment resulting from inadequate representation of the Earth structure in the inversion are generally smaller than those of the earthquakes in the GCMT catalog when perturbing the elastic (Fig. 7a) and the anelastic Earth structure (Fig. 7b) independently. However, a perturbation of 10% in the elastic structure and 75% in the anelastic structure together reproduces the mean and standard deviation of the distribution of the NDC components in the GCMT catalog

(Fig. 7c), making it possible to explain the NDC components in the GCMT catalog as resulting from not accounting for laterally varying Earth structure. Perturbing the elastic structure of the Earth model alone by 10% without perturbing the anelastic structure results in an average NDC component of 19.5%, only slightly smaller than the observed NDC components in the GCMT catalog. However, uncertainties in the anelastic structure are large (Karaoğlu and Romanowicz, 2018) and can reach 75% for seismic waves with periods of 100s as used in this experiment (Dalton and Ekström, 2006).

4 Discussion and Conclusions

Generating synthetic seismograms for the DC components of 25 arbitrarily selected earthquakes in the GCMT catalog using one Earth model and inverting them with another Earth model gives rise to MTs with NDC components because the inversion changes the mechanism to include a substantial NDC component. Perturbing both elastic and anelastic Earth structure yields a distribution of NDC components similar to that of NDC components reported for the earthquakes in the GCMT catalog. This process shows the sensitivity of MTs to the effects of variable Earth structure. This behavior is expected to be similar, but larger, for shorter periods than the > 100 s we present, which is presumably why smaller earthquakes have larger NDC components than larger earthquakes in global MT catalogs.

These results for global datasets are generally similar to those derived for regional data. Stierle et al. (2014b) found that unconstrained MT inversions allowing an isotropic component produce larger NDC compo-

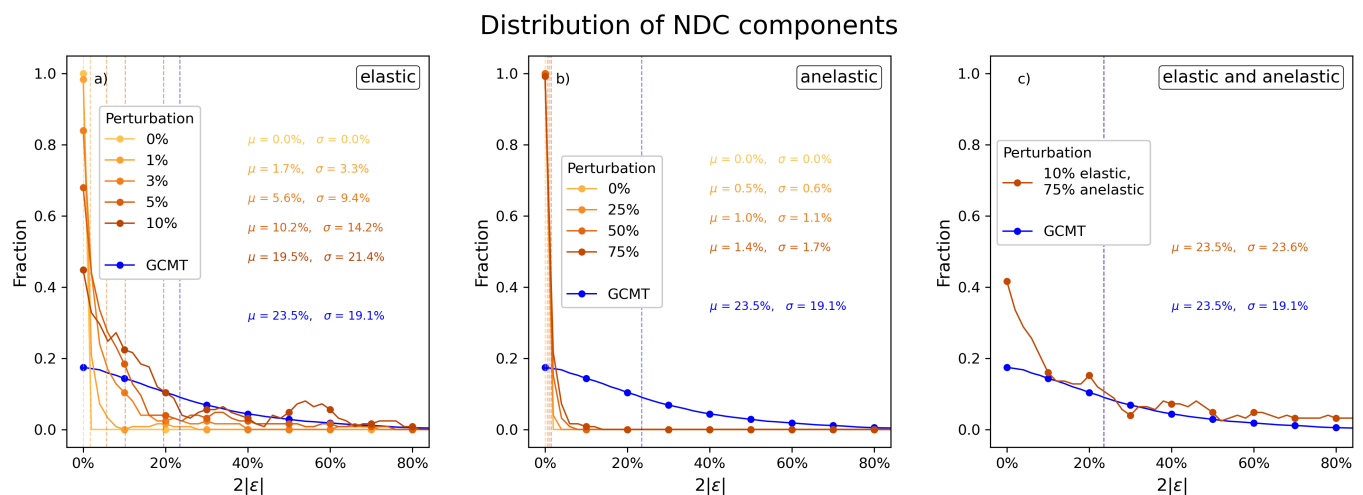


Figure 7 Distribution of non-double couple (NDC) components generated by inverting seismograms generated using a model with perturbed elastic (a) and anelastic (b) structure using unperturbed Preliminary Reference Earth Model (PREM). A combined perturbation of elastic and anelastic structure (c) generally reproduces the distribution of NDC components in the Global Centroid Moment Tensor (GCMT) catalog.

nents than constrained inversions. Stierle et al. (2014a) found that the aftershocks of the M_w 7.4 Izmit earthquake in 1999 had average NDC components of 19.6%. For the earthquakes of a swarm in 1997 in Czech Republic, Vavryčuk (2002) and Horálek et al. (2002) reported a mean deviation from a DC source of 17.3%. These studies found earthquakes with NDC components of up to 57.0% and 49.8%, respectively. The MT inversion in both studies used Green's functions generated for regional 1D Earth models, using the P- and S-wave amplitudes to stabilize the inversion, thus giving confidence that these NDC components represent real source processes.

NDC components of some earthquakes reflect complex source processes differing from slip on a planar fault or the combined effect of DC sources on multiple faults with different geometries. However, the fact that our numerical experiment replicates general features of the pervasive NDC components reported in moment tensor catalogs implies that these components are largely artifacts of the inversions not adequately accounting for the effects of laterally varying Earth structure.

This effect seems similar for the other MT catalogs we examined, which show comparable NDC components. The MTs in all global catalogs were derived using the one-dimensional Earth model PREM. However, the GCMT catalog corrects seismic waveforms for laterally varying Earth structure along the great-circle path of surface waves (Dziewonski et al., 1984). This approach changes the phase spectra, but not the amplitude spectra, and thus does not fully represent the expected effects of 3D structure.

NDC components are often attributed geologic meaning based on their size (Vavryčuk, 2002; Stierle et al., 2014a) without further investigation about their origin. Large NDC components and NDC components of large earthquakes are in fact more reliably determined in MT inversions based on 1D Earth models (Rösler et al., 2023) and are thus more likely to represent real source

processes. However, based on the results of our numerical experiment, the threshold above which they can be considered real source processes based only on their size must be placed at 2σ from their global average of 23.5% at 61.7%, consistent with the results of Rösler et al. (2023). Earthquakes with real, but smaller NDC components exist, but require further knowledge about the geologic setting of the fault rupture occurred on, or knowledge from multiple MT inversions with different Earth models to confirm the significance of NDC components. MT inversions of global catalogs can be improved and artifactual NDC components reduced by using Green's functions generated for a 3D Earth model. However, Šílený and Vavryčuk (2002) found that isotropic and compensated linear-vector dipole (CLVD) components are overestimated for DC sources when inverting events with waveforms recorded in anisotropic structures but assuming isotropy. Therefore, the best estimates of NDC components require a laterally varying Earth model including anisotropy (Hjörleifsdóttir and Ekström, 2010; Sawade et al., 2022).

The results here, combined with the poor correlation between NDC components in different catalogs, suggest that the pervasive NDC components reported in moment tensor catalogs are largely artifacts of the inversions not adequately accounting for the effects of laterally varying Earth structure. More realistic estimates of NDC components will thus require inversion methods that better model the effects of lateral variability which increase computational cost and are less applicable for routinely determined MTs.

Acknowledgements

We thank Emile Okal, Craig Bina, Reece Elling, James Neely, and Molly Gallahue for helpful discussions that improved the manuscript, and for the suggestions made by anonymous reviewers and the handling editor, Stephen Hicks. We thank Brian Shiro and David Wil-

son for comments and handling the USGS approval of this manuscript, and Dara Goldberg and Janet Carter for providing internal reviews. Any use of trade, firm, or product names is for descriptive purposes only and does not imply endorsement by the U.S. Government.

Data and code availability

The Global CMT Project catalog used in this study was downloaded from globalcmt.org. We used the MinEOS software package (Masters et al.), available at geodynamics.org, and station locations of the Global Seismographic Network to generate synthetic seismograms. These data are freely available from the Earthscope Consortium. For the data analysis, we used ObsPy (Beyreuther et al., 2010), and BayesISOLA for the moment tensor inversion, available at github.com/vackar/BayesISOLA.

The EarthScope Consortium is funded through the Seismological Facility for the Advancement of Geoscience (SAGE) Award of the National Science Foundation under Cooperative Agreement EAR-1724509.

The Global Seismographic Network (GSN) is a cooperative scientific facility operated jointly by the Earthscope Consortium, the U.S. Geological Survey (USGS), and the National Science Foundation (NSF), under Cooperative Agreement EAR-1261681.

Competing interests

The authors declare no competing interests.

References

- Aki, K. and Richards, P. G. Quantitative Seismology. *University Science Books*, 2002.
- Ammon, C. J., Lay, T., Velasco, A. A., and Vidale, J. E. Routine estimation of earthquake source complexity: The 18 October 1992 Colombian earthquake. *Bulletin of the Seismological Society of America*, 4(84):1266–1271, 1994. doi: 10.1785/BSSA0840041266.
- Beyreuther, M., Barsch, R., Krischer, L., Megies, T., Behr, Y., and Wassermann, J. ObsPy: A Python toolbox for seismology. *Seismological Research Letters*, 81(3):530–533, 2010. doi: 10.1785/gssrl.81.3.530.
- Cesca, S., Buforn, E., and Dahm, T. Amplitude spectra moment tensor inversion of shallow earthquakes in Spain. *Geophysical Journal International*, 166(2):839–854, 2006. doi: 10.1111/j.1365-246X.2006.03073.x.
- Cohee, B. P. and Beroza, G. C. Slip distribution of the 1992 Landers earthquake and its implications for earthquake source mechanics. *Bulletin of the Seismological Society of America*, 84(3):692–712, 1994. doi: 10.1785/BSSA0840030692.
- Covellone, B. M. and Savage, B. A quantitative comparison between 1D and 3D source inversion methodologies: Application to the Middle East. *Bulletin of the Seismological Society of America*, 102(5):2189–2199, 2012. doi: 10.1785/0120110278.
- Dahlen, F. and Tromp, J. Theoretical global seismology. *Princeton University Press*, 1998.
- Dahlen, F. A. The effect of data windows on the estimation of free oscillation parameters. *Geophysical Journal International*, 2(69):537–549, 1982. doi: 10.1111/j.1365-246X.1982.tb04964.x.
- Dalton, C. A. and Ekström, G. Global models of surface wave attenuation. *Journal of Geophysical Research: Solid Earth*, B5(111), 2006. doi: 10.1029/2005JB003997.
- Domingues, A., Custodio, S., and Cesca, S. Waveform inversion of small-to-moderate earthquakes located offshore southwest Iberia. *Geophysical Journal International*, 192(1):248–259, 2013. doi: 10.1093/gji/ggs010.
- Donner, S., Mustač, M., Hejrani, B., Tkalčić, H., and Igel, H. Seismic moment tensors from synthetic rotational and translational ground motion: Green's functions in 1-D versus 3-D. *Geophysical Journal International*, 223(1):161–179, 2020. doi: 10.1093/gji/g-gaa305.
- Duputel, Z., Rivera, L., Kanamori, H., and Hayes, G. W phase source inversion for moderate to large earthquakes (1990–2010). *Geophysical Journal International*, 2(189):1125–1147, 2018. doi: 10.1111/j.1365-246X.2012.05419.x.
- Dziewonski, A. M. and Anderson, D. L. Preliminary reference Earth model. *Physics of the Earth and Planetary Interiors*, 25(4):297–356, 1981. doi: 10.1016/0031-9201(81)90046-7.
- Dziewonski, A. M., Chou, T. A., and Woodhouse, J. H. Determination of earthquake source parameters from waveform data for studies of global and regional seismicity. *Journal of Geophysical Research: Solid Earth*, B4(86):2825–2852, 1981. doi: 10.1029/JB086iB04p02825.
- Dziewonski, A. M., Franzen, J. E., and Woodhouse, J. H. Centroid-moment tensor solutions for January–March, 1984. *Physics of the Earth and Planetary Interiors*, 4(34):209–219, 1984. doi: 10.1016/0031-9201(84)90062-1.
- Ekström, G., Nettles, M., and Dziewonski, A. The global CMT project 2004–2010: Centroid-moment tensors for 13,017 earthquakes. *Physics of the Earth and Planetary Interiors*, 200–201:1–9, 2012. doi: 10.1016/j.pepi.2012.04.002.
- Ford, S. R., Dreger, D. S., and Walter, W. R. Network sensitivity solutions for regional moment-tensor inversions. *Bulletin of the Seismological Society of America*, 100(5A):1962–1970, 2010. doi: 10.1785/0120090140.
- Frolich, C. Triangle diagrams: ternary graphs to display similarity and diversity of earthquake focal mechanisms. *Physics of the Earth and Planetary Interiors*, 75(1-3):193–198, 1992. doi: 10.1016/0031-9201(92)90130-N.
- Frolich, C. Earthquakes with non-double-couple mechanisms. *Science*, 5160(264):804–809, 1994. doi: 10.1126/science.264.5160.804.
- Gilbert, F. Excitation of the normal modes of the Earth by earthquake sources. *Geophysical Journal International*, 2(22):223–226, 1971. doi: 10.1111/j.1365-246X.1971.tb03593.x.
- Gudmundsson, M. T., Jónsdóttir, K., A., H., Holohan, E. P., Halldórsson, S. A., Ófeigsson, B. G., Cesca, S., Vogfjörð, K. S., Sigmundsson, F., Högnadóttir, T., Einarsson, P., Sigmarsson, O., Jarosch, A. H., Jónasson, K., Magnússon, E., Hreinsdóttir, S., Bagnardi, M., Parks, M. M., Hjörleifsdóttir, V., Pálsson, F., W. T. R., Schöpfer, M. P. J., Heimann, S., Reynolds, H. I., Dumont, S., Bali, E., Gudfinnsson, G. H., Dahm, T., Roberts, M. J., Hensch, M., Belart, J. M. C., Spaans, K., Jakobsson, S., Gudmundsson, G. B., Fridriksdóttir, H. M., Drouin, V., Dürig, T., Adalgeirsdóttir, G., Rishuus, M. S., Pedersen, G. B. M., Van Boeckel, T., Oddsson, B., Pfeffer, M. A., Barsotti, S., Bergsson, B., Donovan, A., Burton, M. R., and Aiuppa, A. Gradual caldera collapse at Bárðarbunga volcano, Iceland, regulated by lateral magma outflow. *Science*, 353(6296), 2016. doi: 10.1126/science.aaf8988.
- Hallo, M. and Gallovič, F. Fast and cheap approximation of Green function uncertainty for waveform-based earthquake source inversions. *Geophysical Journal International*, 207(2):1012–1029, 2016. doi: 10.1093/gji/ggw320.

- Hamling, I. J., Hreinsdóttir, S., Clark, K., Elliott, J., Liang, C., Fielding, E., Litchfield, N., Villamor, P., Wallace, L., Wright, T. J., d'Anastasio, E., Bannister, S., Burbridge, D., Denys, P., Gentle, P., Howarth, J., Mueller, C., Palmer, N., Pearson, C., Power, W., Barnes, P., Barrell, D. J. A., van Dissen, R., Langridge, R., Little, T., Nicol, A., Pettinga, J., Rowland, J., and Stirling, M. Complex multifault rupture during the M_w 7.8 Kaikōura earthquake, New Zealand. *Science*, 356(6334), 2017. doi: 10.1126/science.aam7194.
- Hayes, G. P., Rivera, L., and Kanamori, H. Source inversion of the W-Phase: real-time implementation and extension to low magnitudes. *Seismological Research Letters*, 80(5):817–822, 2009. doi: 10.1785/gssrl.80.5.817.
- Hayes, G. P., Briggs, R. W., Sladen, A., Fielding, E. J., Prentice, C., Hudnut, K., Mann, P., Taylor, F. W., Crone, A. J., Gold, R., Ito, T., and Simons, M. Complex rupture during the 12 January 2010 Haiti earthquake. *Nature Geoscience*, 3(11):800–805, 2010. doi: 10.1038/ngeo977.
- Hejrani, B., Tkalčić, H., and Fichtner, A. Centroid moment tensor catalogue using a 3-D continental scale Earth model: Application to earthquakes in Papua New Guinea and the Solomon Islands. *Journal of Geophysical Research: Solid Earth*, 122(7): 5517–5543, 2017. doi: 10.1002/2017JB014230.
- Henry, C., Woodhouse, J. H., and S., D. Stability of earthquake moment tensor inversions: effect of the double-couple constraint. *Tectonophysics*, 356(1-3):115–124, 2002. doi: 10.1016/S0040-1951(02)00379-7.
- Hingee, M., Tkalčić, H., Fichtner, A., and Sambridge, M. Seismic moment tensor inversion using a 3-D structural model: applications for the Australian region. *Geophysical Journal International*, 184(2):949–964, 2011. doi: 10.1111/j.1365-246X.2010.04897.x.
- Hjörleifsdóttir, V. and Ekström, G. Effects of three-dimensional Earth structure on CMT earthquake parameters. *Physics of the Earth and Planetary Interiors*, 179(3-4):178–190, 2010. doi: 10.1016/j.pepi.2009.11.003.
- Horálek, J., Šílený, J., and Fischer, T. Moment tensors of the January 1997 earthquake swarm in NW Bohemia (Czech Republic): double-couple vs. non-double-couple events. *Tectonophysics*, 1-3(356):65–85, 2002. doi: 10.1016/S0040-1951(02)00377-3.
- Jechumtálová, Z. and Bulant, P. Effects of 1-D versus 3-D velocity models on moment tensor inversion in the Dobrá Voda area in the Little Carpathians region, Slovakia. *Journal of Seismology*, 18:511–531, 2014. doi: 10.1007/s10950-014-9423-6.
- Jechumtálová, Z. and Šílený, J. Point-source parameters from noisy waveforms: Error estimate by Monte-Carlo simulation. *Pure and Applied Geophysics*, 158(9):1639–1654, 2001. doi: 10.1007/PL00001237.
- Julian, B. R. and Sipkin, S. A. Earthquake processes in the Long Valley caldera area, California. *Journal of Geophysical Research: Solid Earth*, 90(B13):11155–11169, 1985. doi: 10.1029/JB090iB13p11155.
- Kagan, Y. Y. 3-D rotation of double-couple earthquake sources. *Geophysical Journal International*, 106(3):709–716, 1991. doi: 10.1111/j.1365-246X.1991.tb06343.x.
- Kanamori, H. and Given, J. W. Analysis of long-period seismic waves excited by the May 18, 1980, eruption of Mount St. Helens - A terrestrial monopole? *Journal of Geophysical Research: Solid Earth*, 87(B7):5422–5432, 1982. doi: 10.1029/JB087iB07p05422.
- Kanamori, H. and Rivera, L. W phase. *Geophysical Research Letters*, 16(20):1691–1694, 1993. doi: 10.1029/93GL01883.
- Kanamori, H., R. L. Source inversion of W-phase: Speeding up seismic tsunami warning. *Geophysical Journal International*, 1(175): 222–238, 2008. doi: 10.1111/j.1365-246X.2008.03887.x.
- Karaoğlu, H. and Romanowicz, B. Inferring global upper-mantle shear attenuation structure by waveform tomography using the spectral element method. *Geophysical Journal International*, 3(213):1536–1558, 2018. doi: 10.1093/gji/ggy030.
- Kawakatsu, H. Enigma of earthquakes at ridge-transform-fault plate boundaries distribution of non-double-couple parameter of Harvard CMT Solutions. *Geophysical Research Letters*, 18(6): 1103–1106, 1991. doi: 10.1029/91GL01238.
- Knopoff, L. and Randall, M. J. The compensated linear-vector dipole: A possible mechanism for deep earthquakes. *Journal of Geophysical Research*, 26(75):4957–4963, 1970. doi: 10.1029/JB075i026p04957.
- Liu, Q., Polet, J., Komatitsch, D., and Tromp, J. Spectral-element moment tensor inversions for earthquakes in southern California. *Bulletin of the Seismological Society of America*, 94(5): 1748–1761, 2004. doi: 10.1785/012004038.
- Masters, G., Woodhouse, J., and Freeman, G. *Computational Infrastructure for Geodynamics*, url: <https://geodynamics.org/cig>.
- McNamara, D. E., Benz, H. M., Herrmann, R. B., Bergman, E. A., Earle, P., Meltzer, A., Withers, M., and Chapman, M. The Mw 5.8 Mineral, Virginia, Earthquake of August 2011 and Aftershock Sequence: Constraints on Earthquake Source Parameters and Fault Geometry. *Bulletin of the Seismological Society of America*, 1(104):40–54, 2013.
- Miller, A. D., Foulger, G. R., and Julian, B. R. Non-double-couple earthquakes 2. Observations. *Reviews of Geophysics*, 36(4): 551–568, 1998. doi: 10.1029/98RG00717.
- Nettles, M. and Ekström, G. Faulting mechanism of anomalous earthquakes near Bárðarbunga Volcano, Iceland. *Journal of Geophysical Research: Solid Earth*, 103(B8):17973–17983, 1998. doi: 10.1029/98JB01392.
- Pang, G., Koper, K. D., Mesimeri, M., Pankow, K. L., Baker, B., Farrell, J., Holt, J., Hale, J. M., Roberson, P., Burlacu, R., Pechmann, J. C., Whidden, K., Holt, M. M., Allamm, A., and DuRoss, C. Seismic analysis of the 2020 Magna, Utah, earthquake sequence: Evidence for a listric Wasatch fault. *Geophysical Research Letters*, 47(18), 2020. doi: 10.1029/2020GL089798.
- Phạm, T. S. and Tkalčić, H. Toward Improving Point-Source Moment-Tensor Inference by Incorporating 1D Earth Model's Uncertainty: Implications for the Long Valley Caldera Earthquakes. *Journal of Geophysical Research: Solid Earth*, 126(11), 2021. doi: 10.1029/2021JB022477.
- Quigley, M. C., Mohammadi, H., and Duffy, B. G. Multi-fault earthquakes with kinematic and geometric rupture complexity: how common? *INQUA Focus Group Earthquake Geology and Seismic Hazards*, 2017.
- Ringler, A. T., Anthony, R. E., Aster, R. C., Ammon, C. J., Arrowsmith, S., Benz, H., Ebeling, C., Frassetto, A., Kim, W.-Y., Koelemeijer, P., Lau, H. C. P., Lekić, V., Montagner, J. P., Richards, P. G., Schaff, D. P., Vallee, M., and Yeck, W. Achievements and prospects of global broadband seismographic networks after 30 years of continuous geophysical observations. *Reviews of Geophysics*, 3(60), 2022. doi: 10.1029/2021RG000749.
- Rodríguez-Cardozo, F., Hjörleifsdóttir, V., K., J., Iglesias, A., Franco, S. I., Geirsson, H., Trujillo-Castrillón, N., and M., H. The 2014–2015 complex collapse of the Bárðarbunga caldera, Iceland, revealed by seismic moment tensors. *Journal of Volcanology and Geothermal Research*, 416, 2021. doi: 10.1016/j.jvolgeores.2021.107275.
- Rösler, B. and Stein, S. Consistency of Non-Double-Couple Components of Seismic Moment Tensors with Earthquake Magnitude and Mechanism. *Seismological Research Letters*, 93(3): 1510–1523, 2022. doi: 10.1785/0220210188.
- Rösler, B., Stein, S., and Spencer, B. D. Uncertainties in Seismic

- Moment Tensors Inferred from Differences Between Global Catalogs. *Seismological Research Letters*, 92(6):3698–3711, 2021. doi: 10.1785/0220210066.
- Rösler, B., Stein, S., and Spencer, B. D. When are Non-Double-Couple Components of Seismic Moment Tensors Reliable? *Seismica*, 2(1), 2023.
- Ross, A., Foulger, G. R., and Julian, B. R. Non-double-couple earthquake mechanisms at the Geysers geothermal area, California. *Geophysical Research Letters*, 23(8):877–880, 1996. doi: 10.1029/96GL00590.
- Rößler, D., Krüger, F., and Rumpker, G. Retrieval of moment tensors due to dislocation point sources in anisotropic media using standard techniques. *Geophysical Journal International*, 169(1): 136–148, 2007. doi: 10.1111/j.1365-246X.2006.03243.x.
- Ruhl, C. J., Morton, E. A., Bormann, J. M., Hatch-Ibarra, R., Ichinose, G., and Smith, K. D. Complex Fault Geometry of the 2020 M_{ww} 6.5 Monte Cristo Range, Nevada, Earthquake Sequence. *Seismological Research Letters*, 92(3):1876–1890, 2021. doi: 10.1785/0220200345.
- Saloor, N. and Okal, E. A. Extension of the energy-to-moment parameter Θ to intermediate and deep earthquakes. *Physics of the Earth and Planetary Interiors*, 274:37–48, 2018. doi: 10.1016/j.pepi.2017.10.006.
- Sandanbata, O., Kanamori, H., Rivera, L., Zhan, Z., Watada, S., and Satake, K. Moment tensors of ring-faulting at active volcanoes: Insights into vertical-CLVD earthquakes at the Sierra Negra caldera, Galápagos Islands. *Journal of Geophysical Research: Solid Earth*, 126(6), 2021. doi: 10.1029/2021JB021693.
- Sawade, L., Beller, S., L. W., and Tromp, J. Global centroid moment tensor solutions in a heterogeneous earth: the CMT3D catalogue. *Geophysical Journal International*, 231(3):1727–1738, 2022. doi: 10.1093/gji/ggac280.
- Scognamiglio, L., Tinti, E., Casarotti, E., Pucci, S., Villani, F., Cocco, M., Magnoni, F., Michelini, A., and Dreger, D. Complex fault geometry and rupture dynamics of the M_w 6.5, 30 October 2016, Central Italy earthquake. *Journal of Geophysical Research: Solid Earth*, 123(4):2943–2964, 2018. doi: 10.1002/2018JB015603.
- Shuler, A., Ekström, G., and Nettles, M. Physical mechanisms for vertical-CLVD earthquakes at active volcanoes. *Journal of Geophysical Research: Solid Earth*, 118(4):1569–1586, 2013a. doi: 10.1002/jgrb.50131.
- Shuler, A., Nettles, M., and Ekström, G. Global observation of vertical-CLVD earthquakes at active volcanoes. *Journal of Geophysical Research: Solid Earth*, 118(1):138–164, 2013b. doi: 10.1029/2012JB009721.
- Šílený, J. Regional moment tensor uncertainty due to mismodeling of the crust. *Tectonophysics*, 383(3-4):133–147, 2004. doi: 10.1016/j.tecto.2003.12.007.
- Šílený, J., Campus, P., and Panza, G. F. Seismic moment tensor resolution by waveform inversion of a few local noisy records - I. Synthetic tests. *Geophysical Journal International*, 126(3): 605–619, 1996. doi: 10.1111/j.1365-246X.1996.tb04693.x.
- Sipkin, S. A. Interpretation of non-double-couple earthquake mechanisms derived from moment tensor inversion. *Journal of Geophysical Research: Solid Earth*, B1(91):531–547, 1986. doi: 10.1029/JB091iB01p00531.
- Stierle, E., Bohnhoff, M., and Vavryčuk, V. Resolution of non-double-couple components in the seismic moment tensor using regional networks-II: application to aftershocks of the 1999 M_w 7.4 Izmit earthquake. *Geophysical Journal International*, 3(169):1878–1888, 2014a. doi: 10.1093/gji/ggt503.
- Stierle, E., Vavryčuk, V., Šílený, J., and Bohnhoff, M. Resolution of non-double-couple components in the seismic moment tensor using regional networks-I: a synthetic case study. *Geophysical Journal International*, 3(169):1869–1877, 2014b. doi: 10.1093/gji/ggt502.
- Tréhu, A. M., Nábělek, J. L., and Solomon, S. C. Source characterization of two Reykjanes Ridge earthquakes: Surface waves and moment tensors; P waveforms and nonorthogonal nodal planes. *Journal of Geophysical Research: Solid Earth*, B3(86): 1701–1724, 1981. doi: 10.1029/JB086iB03p01701.
- Vackář, Burjáněk, J., Gallovič, F., Zahradník, J., and Clinton, J. Bayesian ISOLA: new tool for automated centroid moment tensor inversion. *Geophysical Journal International*, 2(210): 693–705, 2017. doi: 10.1093/gji/ggx158.
- Vasyura-Bathke, H., Dettmer, J., Dutta, R., Mai, P. M., and Jons-son, S. Accounting for theory errors with empirical Bayesian noise models in nonlinear centroid moment tensor estimation. *Geophysical Journal International*, 225(2):1412–1431, 2021. doi: 10.1093/gji/ggab034.
- Vavryčuk, V. Non-double-couple earthquakes of 1997 January in West Bohemia, Czech Republic: evidence of tensile faulting. *Geophysical Journal International*, 2(149):364–373, 2002. doi: 10.1046/j.1365-246X.2002.01654.x.
- Vera Rodriguez, I., Gu, Y. J., and Sacchi, M. D. Resolution of seismic-moment tensor inversions from a single array of receivers. *Bulletin of the Seismological Society of America*, 101(6):2634–2642, 2011. doi: 10.1785/0120110016.
- Šílený, J. and Vavryčuk, V. Can unbiased source be retrieved from anisotropic waveforms by using an isotropic model of the medium? *Tectonophysics*, 1-3(356):125–138, 2002. doi: 10.1016/S0040-1951(02)00380-3.
- Wald, D. J. and Heaton, T. H. Spatial and temporal distribution of slip for the 1992 Landers, California, earthquake. *Bulletin of the Seismological Society of America*, 84(3):668–691, 1994. doi: 10.1785/BSSA0840030668.
- Wang, X. and Zhan, Z. Moving from 1-D to 3-D velocity model: automated waveform-based earthquake moment tensor inversion in the Los Angeles region. *Geophysical Journal International*, 220(1):218–234, 2020. doi: 10.1093/gji/ggz435.
- Yang, J., Zhu, H., Lay, T., Niu, Y., Ye, L., Lu, Z., Luo, B., Kanamori, H., Huang, J., and Li, Z. Multi-fault opposing-dip strike-slip and normal-fault rupture during the 2020 M_w 6.5 Stanley, Idaho earthquake. *Geophysical Research Letters*, 48(10), 2021. doi: 10.1029/2021GL092510.
- Zhu, L. and Zhou, X. Seismic moment tensor inversion using 3D velocity model and its application to the 2013 Lushan earthquake sequence. *Physics and Chemistry of the Earth, Parts A/B/C*, 95: 10–18, 2016. doi: 10.1016/j.pce.2016.01.002.

The article *Apparent Non-Double-Couple Components as Artifacts of Moment Tensor Inversion* © 2024 by Boris Rösler is licensed under CC BY 4.0.